HHS Public Access

Author manuscript

Stem Cell Rev Rep. Author manuscript; available in PMC 2022 August 01.

Published in final edited form as:

Stem Cell Rev Rep. 2021 August ; 17(4): 1446–1455. doi:10.1007/s12015-021-10118-w.

Roles of A-kinase anchor protein 12 in astrocyte and oligodendrocyte precursor cell in postnatal corpus callosum

Hajime Takase[1,2], **Gen Hamanaka**[1], **Ryo Ohtomo**[1], **Ji Hyun Park**[1], **Kelly K. Chung**[1], **Irwin H. Gelman**[3], **Kyu-Won Kim**[4], **Josephine Lok**[1,5], **Eng H. Lo**[1], **Ken Arai**[1,*]

[1]Neuroprotection Research Laboratory, Departments of Radiology and Neurology, Massachusetts General Hospital and Harvard Medical School, Charlestown, MA, USA

[2]Department of Neurosurgery, Graduate School of Medicine, Yokohama City University, Yokohama, Japan

[3]Department of Cancer Genetics and Genomics, Roswell Park Comprehensive Cancer Center, Buffalo, NY, USA

[4]College of Pharmacy and Research Institute of Pharmaceutical Sciences, Seoul National University, Seoul, 08826 Republic of Korea

[5]Department of Pediatrics, Pediatric Critical Care Medicine, Massachusetts General Hospital, Boston, USA

Abstract

The formation of the corpus callosum in the postnatal period is crucial for normal neurological function, and clinical genetic studies have identified an association of 6q24–25 microdeletion in this process. However, the mechanisms underlying corpus callosum formation and its critical gene(s) are not fully understood or identified. In this study, we examined the roles of AKAP12 in postnatal corpus callosum formation by focusing on the development of glial cells, because *AKAP12* is coded on 6q25.1 and has recently been shown to play roles in the regulations of glial function. In mice, the levels of AKAP12 expression was confirmed to be larger in the corpus

*Corresponding author: Ken Arai, Neuroprotection Research Laboratory, MGH East 149-2401, Charlestown, MA 02129, USA. Tel: +1.617.724.9503, karai@partners.org.

Author contributions:
Collection of data: HT, GH, RO
Data analysis: HT, JH, RO, KA
Manuscript writing: HT, KKC, JL, EHL, KA
Interpretation: HT, JHP, KKC, IHG, KWK, JL, EHL, KA
Conception and design: HT, EHL, KA
Funding acquisition: HT, JL, EHL, KA
Final approval of manuscript: HT, GH, RO, JHP, KKC, IHG, KWK, JL, EHL, KA

Conflicts of interest/Competing interests: The authors declare no competing or financial interests.

Declarations:
Ethics approval: All experimental procedures followed NIH guidelines and were approved by the Massachusetts General Hospital Institutional Animal Care and Use Committee.
Consent to participate: Not applicable
Consent for publication: Not applicable
Availability of data and material: Derived data supporting the findings of this study are available from the corresponding author upon request.
Code availability: Not applicable

callosum compared to the cortex, and AKAP12 levels decreased with age both in the corpus callosum and cortex regions. In addition, astrocytes expressed AKAP12 in the corpus callosum after birth, but oligodendrocyte precursor cells (OPCs), another major type of glial cell in the developing corpus callosum, did not. Furthermore, compared to wild types, *Akap12* knockout mice showed smaller numbers of both astrocytes and OPCs, along with slower development of corpus callosum after birth. These findings suggest that AKAP12 signaling may be required for postnatal glial formation in the corpus callosum through cell- and non-cell autonomous mechanisms.

Keywords

A-kinase anchor protein 12; white matter; astrocytes; oligodendrocyte precursor cells; postnatal development; brain

Introduction:

White matter is composed of axonal bundles surrounded by myelin, which connect and synchronize neural activity between various cortical areas. Among the white matter structures in the brain, the corpus callosum is the largest, with millions of nerve fibers that form a thick commissural tract connecting the cerebral hemispheres. The number of these fibers is determined at birth; however, the structural and functional maturation of the corpus callosum continues during the postnatal period. Because of its central role in neurological function, the molecular mechanisms that promote or impede functional maturation of the corpus callosum need to be examined to understand the processes of CNS development.

During embryonic and fetal development, chromosomal abnormality is one of the major causes of agenesis (or hypoplasia/dysgenesis) of the corpus callosum (ACC). Although the discovery of genotype–phenotype correlations has been constrained by the limitations of standard cytogenetic techniques, an important observation is that phenotype varies with some correlation to specific deleted regions [1]. Among chromosomal abnormalities, a rare interstitial deletion, 6q deletion, has been documented to be “disease causing” with observable clinical phenotypes, such as dysmorphic features, intellectual disabilities, upper limb malformations, microcephaly and brain abnormalities including ACC [2]. Other studies with a higher resolution of gene identification suggest that a 6q24–25 microdeletion may contribute to CNS features of 6q deletion [3]. Nevertheless, the definitive genetic lesions that result in abnormal postnatal corpus callosum formation remain unknown.

AKAP12 (A-kinase anchor protein 12; also called SSeKS or Gravin) has emerged as a potential candidate gene in the postnatal development of the corpus callosum. AKAP12 is a scaffolding protein that is known as a tumor suppressor that regulates oncogenic pathways through the selective binding of signaling proteins, such as PKA or PKC [4, 5]. In the CNS, it has been reported that AKAP12 regulates vascular development and differentiation [6–9]. Furthermore, a recent study using in-vivo and in-vitro experiments demonstrated a critical role of AKAP12 in the function of oligodendroglial cells in adult cerebral white matter [10]. Along with these reports of the role of AKAP12 in the CNS, because the locus of human *AKAP12* is located on distal chromosome 6q25.1, the chromosome region that has been

associated with ACC, we hypothesized that AKAP12 may regulate corpus callosum formation in the postnatal period. In this study, therefore, we compared *Akap12* knockout mice with wild-type mice to elucidate the roles of AKAP12 in glial formation in the postnatal corpus callosum.

Materials and Methods:

Animals –

All experimental procedures followed NIH guidelines and were approved by the Massachusetts General Hospital Institutional Animal Care and Use Committee. *Akap12* KO mice of C57BL/6 background were provided from the Gelman Lab at Roswell Park Comprehensive Cancer Center [11] and were maintained/expanded in the animal facility at Massachusetts General Hospital. Protocols for the genotyping of *Akap12* KO mouse lines are as previously described [10]. After screening DNA samples (see the representative images in Supplementary Figure S1a), mice were used for experiments. After each experiment, the genotype of each mouse was re-confirmed by measuring protein levels of AKAP12 in the brain homogenate (see the representative images in Supplementary Figure S1b–c). We used both male and female mice from our mouse colony, and a total of 104 mice (WT; n = 41, $Akap12^{+/-}$; n = 31, $Akap12^{-/-}$; n = 32) were used in this study. Of these, 92 mice (WT; n = 29, $Akap12^{+/-}$; n = 31, $Akap12^{-/-}$; n = 32) were from 16 female $Akap12^{+/-}$mice crossed with male $Akap12^{+/-}$ mice. Each set of littermates was allocated to the same experiment. The other 12 WT male mice used for the protein expression experiment (for Figure 1a–b) were from another cohort. Detailed information of animal numbers for each experiment is presented in our supplementary information.

Measurement of body length –

For the measurement of body length, a neutral posture was captured by digital camera from above. Then, the length from the nasal tip to the tail base was traced and measured using ImageJ (NIH) by an operator who was blinded to the group allocation.

Western blot –

Brains were removed following transcardial perfusion with 2-mL/g body-weight of ice-cold 0.1M phosphate-buffered saline (PBS). Tissue samples of whole brain (P0), cerebral cortex and corpus callosum (postnatal 2-weeks, 2- and 8- months) were dissected in NP40 cell lysis buffer (MyBiosource). After centrifuge and aspiration of the supernatant, digested samples with equal volumes of LDS sample buffer including reducing agent (NuPage) were heated at 70°C for 10 min. Seven μg of each sample were then loaded onto 4–12% Bis-Tris gels. After electrophoresis and transfer to nitrocellulose membranes, the membranes were blocked in 5% skim milk with Tris-buffered saline (TBS) containing 0.1% Tween-20. Afterwards, they were incubated with a primary antibody against AKAP12 (1:1,000, obtained from the Gelman Lab) and β-actin (1:10,000, A5441, Sigma-Aldrich). Then, membranes were processed with HRP-conjugated secondary antibodies (1:2,000, Jackson Immunoresearch Laboratories) for 1 h at room temperature (RT) and visualized by enhanced chemiluminescence (SuperSignal™ West Femto Maximum Sensitivity Substrate,

ThermoFisher Scientific). Visualized bands were semi-quantified using ImageJ by an operator who was blinded to the group allocation.

Immunohistochemical procedures and quantification –

On postnatal day 0 (P0) and 14 (P14), 15 mice per time point received transcardiac perfusion with ice-cold PBS. Removed brains were then stored in −80°C until use. Fresh frozen brains were embedded with optimal cutting temperature (OCT) compound. Twenty-μm thick coronal sections at the level of the anterior third of the corpus callosum were prepared for immunostaining using cryostat CM1520 (Leica). Only sections with a circular shape of the anterior commissure at the ventral edge of the lateral ventricle (corresponding to the area 0.8–1.0 mm anterior to bregma in the adult mouse, http://atlas.brain-map.org/atlas?atlas=2&plate=100883869#atlas=2&plate=100883888&resolution=33.45&x=7756&y=3956&zoom=-4) were included in this study (Figure 4a). The sections were fixed with methanol for 12 min at −20°C. After being washed with PBS three times, they were blocked with 3% bovine serum albumin (BSA) in PBS for 1 hour at RT. The sections were then incubated in 1% BSA in PBS containing anti-AKAP12 (1:500, Obtained from the Gelman Lab), anti-GFAP (1:500, #130300, Invitrogen, USA), anti-PDGFRα (1:100, AF1062, R&D systems, USA), and anti-S100 (1:200, ab4066, Abcam, USA) at 4°C overnight. After that, they were incubated with secondary antibodies (1:500, Jackson Immunoresearch Laboratories) for 1h at RT. Finally, the sections were sufficiently washed with PBS and covered with ProLong™ Gold mounting solution with DAPI (P36930, ThermoFisher Scientific, USA). Stained sections were observed with fluorescent microscope (Nikon) and scanned with Retiga™ 2000R Fast 1394 Digital Camera. For quantification of cell numbers of PDGFRα and area of $GFAP^+$ and $S100^+$, we first set the region of interest (ROI) of a 200 × 100 μm rectangle in the center of CC at the midline, as shown in the diagram in Figure 4b–c and Supplementary Figure 2. Within the ROI, cell numbers were counted manually, and the area of positive cells was measured using ImageJ software (NIH). For further assessment of $GFAP^+$ area and cell numbers of PDGFRα in CC, we set 4 ROIs by drawing a 100 μm square in the bilateral side (see the diagram in Supplementary Figure S3 and Supplementary Figure S4) as follows - [ROI a]: the center of the corpus callosum at the midline, [ROI b]: the mid-point between [ROI a] and [ROI c], [ROI c]: the center of the lateral ventricle on the lateral axis (for P0) or the lateral edge of the lateral ventricle on the lateral axis (for P14), and [ROI d]: the highest point on the ventral-dorsal axis. GFAP with DAPI was used to demarcate the boundary between the corpus callosum and other surrounding structures (see the diagram in Figure 3a). The thickness of the cerebral cortex was defined from the dorsal edge to the ventral edge beside the interhemispheric fissure (see the diagram in Figure 3a). The quantification was conducted by an operator who was blinded to the group allocation.

Statistics –

Statistical analyses were performed with Prism 8 (Graphpad, USA). Statistical significance was evaluated using 1- or 2-way (repeated-measures) ANOVA with post-hoc test for multiple comparisons, as appropriate. Data are expressed as mean plus and/or minus S.D. A p value of < 0.05 was considered statistically significant.

Results:

Spatio-temporal patterns of AKAP12 expression in mouse brain:

We first examined the spatio-temporal patterns of AKAP12 expression in postnatal mouse brains. AKAP12 protein expression is greater in the corpus callosum compared to the cerebral cortex, and its expression levels gradually decreased with age (Figure 1a–b), which highlights the importance of examining the roles of AKAP12 in the postnatal corpus callosum. We then examined which cell type(s) expressed AKAP12 in the postnatal corpus callosum. Immunostaining of mouse coronal brain sections showed that GFAP-positive astrocytes express AKAP12 at postnatal days 0 and 14 (Figure 2a). On the other hand, AKAP12 signal was not observed in PDGFRα-positive OPCs, another type of major glial cell in the developing corpus callosum (Figure 2b).

AKAP12 contributes to corpus callosum formation in post-natal development:

To investigate the roles of AKAP12 in the corpus callosum after birth, *Akap12* homozygous (*Akap12*$^{-/-}$) or heterozygous (*Akap12*$^{+/-}$) knockout mice were compared with wild type (WT) littermates (Supplementary Figure S1). We first examined whether *Akap12* deficiency influenced physical parameters, such as body length and weight. Among the 3 genotypes, there were no significant differences in body length at 2 weeks of age or body weight at a later stage (e.g. age of 13 weeks) (Supplementary Figure S1d–e). We next assessed how AKAP12 is involved in the postnatal development of cerebral white matter (corpus callosum) with a focus on the midline callosal formation, wherein glial cells play a crucial role through the expression of guidance molecules [12]. At the anterior third level of the corpus callosum in the coronal section of neonatal mouse brains (e.g. corresponding to the area 0.8–1.0 mm anterior to bregma in the adult mouse), the callosal and cortical thickness of P0 and P14 were compared between the 3 genotypes (Figure 3a). Cortical thickness did not significantly differ between the 3 genotypes at both ages (Figure 3b); but importantly, the thickness of the corpus callosum was significantly greater in WT mice compared to that of *Akap12*$^{+/-}$ or *Akap12*$^{-/-}$ mice (Figure 3c–d). Furthermore, the ratio between callosal thickness and cortical thickness was also significantly greater in WT mice compared to *Akap12*$^{-/-}$ mice (Figure 3e).

Cell- and non-cell-autonomous mechanisms of AKAP12 in glial development:

Finally, we investigated whether AKAP12 expression affected the number of glial cells, i.e. astrocytes and OPCs, in the postnatal corpus callosum. Using the coronal brain sections from WT, *Akap12*$^{+/-}$, and *Akap12*$^{-/-}$ mice (Figure 4a), we confirmed that at the midline of the corpus callosum, *Akap12* deficiency resulted in a smaller number of astrocytes (assessed by the total area of astrocyte markers GFAP or S100beta) at postnatal days 0 and 14 (Figure 4b–e, Supplementary Figure S2). In addition to the midline area of the corpus callosum region, the paramedial areas of the corpus callosum were also found to contain fewer GFAP-positive astrocytes in *Akap12* KO mice on postnatal days 0 and 14 (Supplementary Figure S3). Similarly, a smaller number of PDGFRα-positive OPCs was seen in the midline area of the postnatal corpus callosum of *Akap12* KO mice (Figure 4b–e), and again, the difference in OPC numbers between WT and KO mice was also confirmed in the paramedial areas (Supplementary Figure S4). In addition, the decrease in astrocytes and OPCs in *Akap12*

deficient mice was accompanied by a reduction in the total cell number in the corpus callosum in these mice (Figure 4f).

Discussion:

In this study, we demonstrate that (i) AKAP12 expression level varies according to brain region and age after birth, (ii) AKAP12 expression is observed in GFAP-positive astrocytes but not in PDGFRα-positive OPCs in the postnatal corpus callosum, and (iii) the numbers of astrocytes and OPCs in the postnatal corpus callosum are decreased by *Akap12* deficiency. The observations that the AKAP12 signal is co-localized with an astrocyte marker (Figure 2) and that astrocyte development was decreased by *Akap12* deficiency (Figure 4 and Supplementary Figures S2–3) suggest that astrocytic-AKAP12 contributes to postnatal structural development of the corpus callosum. On the other hand, PDGFRα-positive OPCs in the postnatal corpus callosum did not express AKAP12 even in WT mice (Figure 2), while the number of OPCs was decreased in *Akap12* knockout mice (Figure 4 and Supplementary Figure S4). These findings about the roles of AKAP12 in cell- and non-cell autonomous mechanisms of glial development provide further insights into the cellular mechanisms of corpus callosum formation after birth.

It is now widely accepted that astrocytes play important roles in the postnatal formation of the corpus callosum. In the postnatal corpus callosum, astrocytes maintain the homeostasis of their microenvironment through sensing, integrating, and responding to synaptic activity [13–17]. Besides the fact that midline glia - mainly $GFAP^+$ astrocytes - play a central role in callosal formation via expression of guidance molecules [18–20], another notable role of the astrocyte is its bidirectional interaction with OPCs through the exchange of secreted soluble factors [21–25]. For example, astrocyte-derived PDGF-AA is a positive regulator of OPCs in the postnatal period [26], and astrocytic BDNF supports compensatory OPC activation after white matter damage in the adult brain [27]. The present study lacks direct evidence for AKAP12-related astrocyte-OPC interactions; however, because AKAP12 deficiency caused decreased numbers of astrocytes in the corpus callosum, it is possible that AKAP12 deficiency may result in decreased levels of astrocyte-derived trophic factors for OPCs. In addition, AKAP12 has been reported to regulate the release of soluble factors in the CNS [7, 28]. Therefore, future research regarding the modulation of the astrocytic secretome by AKAP12 signaling will help us understand the astrocyte-OPC interaction in corpus callosum development.

Another important finding of this study is that *Akap12* deficiency appears to be involved in developmental aberrations, which result in ACC. The critical genes responsible for ACC have not yet been characterized in the clinical setting, despite remarkable progress in the molecular science of corpus callosum development. Over the last decades, however, 6q deletion, which is a rare interstitial deletion of the long arm of chromosome 6, has been documented as a possible cause of several brain abnormalities, including ACC [2, 29]. With recent technical advances in high resolution cytogenetics studies, 6q24–25 microdeletion is now recognized as a specific etiology for the representative CNS features of 6q deletion syndrome, such as microcephaly, developmental delay, dysmorphic features, hearing loss or ACC [3, 30–32]. The finding that *Akap12* knockout mice exhibited slower corpus callosum

formation (Figure 3) supports the concept that the *Akap12* gene, which is coded on 6q25.1 in humans, is indeed a critical determinant for ACC. On the other hand, Nagamani et al presented 4 cases of 6q25.2–3 microdeletion with demonstrable features of the 6q deletion syndrome, and ACC was only confirmed in 2 of these 4 cases [3]; also, only 3 out of 8 cases of 6q25.1–3 deletion covering the *AKAP12* locus showed ACC (Supplementary Figure S5) [3, 31–40]. These discrepancies suggest the presence of compensatory mechanisms which support corpus callosum formation under the conditions of 6q25.2–3 microdeletion. Future studies about how combinational deficiencies of genes encoded in the 6q25.3 segment lead to compensatory effects in corpus callosum formation in *Akap12* knockout mice could shed light on the pathological mechanisms and genetic background of ACC. In addition, we may also need to consider the synteny of *AKAP12*. The mouse *Akap12* is on mouse chrom. 10 in a region syntenic to human 6q24–25.1. Some genes downstream of *Akap12*, such as *ESR*, are still on mouse chromosome 10, but others, such as *SCAF8*, are no longer syntenic, i.e. *SCAF8* is on mouse chrom. 17. Hence, future investigations into the mechanisms by which the loss of *Akap12* in mice leads to the downregulation of other ACC-regulating gene functions would provide a deeper understanding of the pathological mechanisms of ACC.

In this study, our data lend support to our hypothesis that AKAP12 plays an active role in glial formation (e.g. astrocytes and OPCs) in the postnatal corpus callosum. However, there are some caveats and limitations, which need to be carefully examined in future studies. First, our current study focused on the roles of AKAP12 in glial development in the postnatal corpus callosum, so our experiments did not place emphasis on the process of axonal tract and myelin sheath formation. However, the formation of myelinated axons is a major indispensable process for corpus callosum during development. Although it is technically difficult to assess myelin proteins in developing corpus callosum partly because their expression levels are low, in order to fully understand the roles of AKAP12 in corpus callosum development, we need to compare axonal tract and myelin sheath formation between WT and *Akap12* KO mice in the next series of experiments. Second, we examined glial formation only in postnatal brains, which does not reflect events in the embryonic stage. Previous studies have demonstrated that perinatal formation of glial cells, including astrocytes, leads to postnatal synaptogenesis and outgrowth of axonal growth cones via secreting guidance molecules [16]. Therefore, future studies are needed to compare glial formation in the prenatal brain between wildtype and *Akap12* KO mice. Third, to understand the pathological mechanisms of ACC, we may also need to pay attention to vascular/BBB development because cerebral vasculature undergoes substantial structural and functional changes during development [41]. Thus far, there is no direct evidence that ACC is accompanied with vascular/BBB dysfunction. However, because astrocytes/OPCs are known to support BBB function [42–44] and because AKAP12 also contributes to BBB tightness [7], it is worthwhile testing a hypothesis that ACC may lead to vascular/BBB dysfunction in corpus callosum through AKAP12-related mechanisms. Finally, we did not examine whether other brain cell types besides astrocytes expressed AKAP12 in the developing brain. Past studies showed that AKAP12 may be expressed in endothelial cells, myelinating oligodendrocytes, and pericytes [6, 28]. In addition, it is still undetermined whether microglia express AKAP12. To understand the cell- and non-cell autonomous mechanisms of AKAP12 in corpus callosum development, we will carefully examine the cell specificity

of AKAP12 expression, and ultimately, the usage of cell-specific *Akap12* deficient mouse lines would be required to assess the mechanisms of AKAP12-related cell-cell interaction for future studies.

In summary, our present study demonstrates that AKAP12 contributes to postnatal corpus callosum formation by increasing the numbers of astrocytes and OPCs. AKAP12 expression was observed in astrocytes, but not in OPCs. Therefore, AKAP12-dependent glial development may depend on both cell-autonomous (astrocytic AKAP12 regulates astrocyte development) and non-cell-autonomous (OPC development is regulated by AKAP12-expressing neighboring cells, such as astrocytes) mechanisms. Our data points to AKAP12 as a likely candidate in the subset of genes responsible for ACC. Future translational studies regarding AKAP12-mediated mechanisms in postnatal corpus callosum formation would provide insights into therapeutic options for ACC.

Supplementary Material

Refer to Web version on PubMed Central for supplementary material.

Acknowledgements:

We thank Mr. Yohei Kuyama, Mr. Naoki Kirihata, and Ms. Nozomi Suzuki for help with genotyping and assistance of some measurements.

Funding: National Institutes of Health, Research Abroad from the Japan Brain Foundation, Mochida Memorial Foundation for Medical and Pharmaceutical Research, the Rotary Foundation Global Scholarship Grants (GG1759314, GG1876795), and the Global Core Research Center Program (GCRC, 2011-0030001) through the National Research Foundation of Korea.

References:

1. Klein OD; Cotter PD; Moore MW; Zanko A; Gilats M; Epstein CJ; Conte F; Rauen KA, Interstitial deletions of chromosome 6q: genotype-phenotype correlation utilizing array CGH. Clin Genet 2007, 71, (3), 260–6. [PubMed: 17309649]
2. Rosenfeld JA; Amrom D; Andermann E; Andermann F; Veilleux M; Curry C; Fisher J; Deputy S; Aylsworth AS; Powell CM; Manickam K; Heese B; Maisenbacher M; Stevens C; Ellison JW; Upton S; Moeschler J; Torres-Martinez W; Stevens A; Marion R; Pereira EM; Babcock M; Morrow B; Sahoo T; Lamb AN; Ballif BC; Paciorkowski AR; Shaffer LG, Genotype-phenotype correlation in interstitial 6q deletions: a report of 12 new cases. Neurogenetics 2012, 13, (1), 31–47. [PubMed: 22218741]
3. Nagamani SC; Erez A; Eng C; Ou Z; Chinault C; Workman L; Coldwell J; Stankiewicz P; Patel A; Lupski JR; Cheung SW, Interstitial deletion of 6q25.2-q25.3: a novel microdeletion syndrome associated with microcephaly, developmental delay, dysmorphic features and hearing loss. Eur J Hum Genet 2009, 17, (5), 573–81. [PubMed: 19034313]
4. Xia W; Unger P; Miller L; Nelson J; Gelman IH, The Src-suppressed C kinase substrate, SSeCKS, is a potential metastasis inhibitor in prostate cancer. Cancer Res 2001, 61, (14), 5644–51. [PubMed: 11454719]
5. Gelman IH, Suppression of tumor and metastasis progression through the scaffolding functions of SSeCKS/Gravin/AKAP12. Cancer Metastasis Rev 2012, 31, (3–4), 493–500. [PubMed: 22684366]
6. Cha JH; Wee HJ; Seo JH; Ahn BJ; Park JH; Yang JM; Lee SW; Kim EH; Lee OH; Heo JH; Lee HJ; Gelman IH; Arai K; Lo EH; Kim KW, AKAP12 mediates barrier functions of fibrotic scars during CNS repair. PLoS One 2014, 9, (4), e94695. [PubMed: 24760034]

7. Lee SW; Kim WJ; Choi YK; Song HS; Son MJ; Gelman IH; Kim YJ; Kim KW, SSeCKS regulates angiogenesis and tight junction formation in blood-brain barrier. Nat Med 2003, 9, (7), 900–6. [PubMed: 12808449]
8. Choi YK; Kim JH; Kim WJ; Lee HY; Park JA; Lee SW; Yoon DK; Kim HH; Chung H; Yu YS; Kim KW, AKAP12 regulates human blood-retinal barrier formation by downregulation of hypoxia-inducible factor-1alpha. J Neurosci 2007, 27, (16), 4472–81. [PubMed: 17442832]
9. Cha JH; Wee HJ; Seo JH; Ahn BJ; Park JH; Yang JM; Lee SW; Lee OH; Lee HJ; Gelman IH; Arai K; Lo EH; Kim KW, Prompt meningeal reconstruction mediated by oxygen-sensitive AKAP12 scaffolding protein after central nervous system injury. Nat Commun 2014, 5, 4952. [PubMed: 25229625]
10. Maki T; Choi YK; Miyamoto N; Shindo A; Liang AC; Ahn BJ; Mandeville ET; Kaji S; Itoh K; Seo JH; Gelman IH; Lok J; Takahashi R; Kim KW; Lo EH; Arai K, A-Kinase Anchor Protein 12 Is Required for Oligodendrocyte Differentiation in Adult White Matter. Stem Cells 2018, 36, (5), 751–760. [PubMed: 29314444]
11. Akakura S; Huang C; Nelson PJ; Foster B; Gelman IH, Loss of the SSeCKS/Gravin/AKAP12 gene results in prostatic hyperplasia. Cancer research 2008, 68, (13), 5096–103. [PubMed: 18593908]
12. Unni DK; Piper M; Moldrich RX; Gobius I; Liu S; Fothergill T; Donahoo AL; Baisden JM; Cooper HM; Richards LJ, Multiple Slits regulate the development of midline glial populations and the corpus callosum. Dev Biol 2012, 365, (1), 36–49. [PubMed: 22349628]
13. Zhang Y; Barres BA, Astrocyte heterogeneity: an underappreciated topic in neurobiology. Curr Opin Neurobiol 2010, 20, (5), 588–94. [PubMed: 20655735]
14. Yang Y; Higashimori H; Morel L, Developmental maturation of astrocytes and pathogenesis of neurodevelopmental disorders. J Neurodev Disord 2013, 5, (1), 22. [PubMed: 23988237]
15. Sofroniew MV; Vinters HV, Astrocytes: biology and pathology. Acta Neuropathol 2010, 119, (1), 7–35. [PubMed: 20012068]
16. Reemst K; Noctor SC; Lucassen PJ; Hol EM, The Indispensable Roles of Microglia and Astrocytes during Brain Development. Front Hum Neurosci 2016, 10, 566. [PubMed: 27877121]
17. Allen NJ; Lyons DA, Glia as architects of central nervous system formation and function. Science 2018, 362, (6411), 181–185. [PubMed: 30309945]
18. Islam SM; Shinmyo Y; Okafuji T; Su Y; Naser IB; Ahmed G; Zhang S; Chen S; Ohta K; Kiyonari H; Abe T; Tanaka S; Nishinakamura R; Terashima T; Kitamura T; Tanaka H, Draxin, a repulsive guidance protein for spinal cord and forebrain commissures. Science 2009, 323, (5912), 388–93. [PubMed: 19150847]
19. Shu T; Richards LJ, Cortical axon guidance by the glial wedge during the development of the corpus callosum. The Journal of neuroscience : the official journal of the Society for Neuroscience 2001, 21, (8), 2749–58. [PubMed: 11306627]
20. Sanchez-Camacho C; Ortega JA; Ocana I; Alcantara S; Bovolenta P, Appropriate Bmp7 levels are required for the differentiation of midline guidepost cells involved in corpus callosum formation. Dev Neurobiol 2011, 71, (5), 337–50. [PubMed: 21485009]
21. Barres BA; Schmid R; Sendnter M; Raff MC, Multiple extracellular signals are required for long-term oligodendrocyte survival. Development (Cambridge, England) 1993, 118, (1), 283–95.
22. Moore CS; Abdullah SL; Brown A; Arulpragasam A; Crocker SJ, How factors secreted from astrocytes impact myelin repair. Journal of neuroscience research 2011, 89, (1), 13–21. [PubMed: 20857501]
23. Durand B; Raff M, A cell-intrinsic timer that operates during oligodendrocyte development. Bioessays 2000, 22, (1), 64–71. [PubMed: 10649292]
24. Miyagi M; Mikawa S; Sato T; Hasegawa T; Kobayashi S; Matsuyama Y; Sato K, BMP2, BMP4, noggin, BMPRIA, BMPRIB, and BMPRII are differentially expressed in the adult rat spinal cord. Neuroscience 2012, 203, 12–26. [PubMed: 22202460]
25. Arai K; Lo E, Astrocytes protect oligodendrocyte precursor cells via MEK/ERK and PI3K/Akt signaling. Journal of neuroscience research 2010, 88, (4), 758–821. [PubMed: 19830833]
26. Raff MC; Lillien LE; Richardson WD; Burne JF; Noble MD, Platelet-derived growth factor from astrocytes drives the clock that times oligodendrocyte development in culture. Nature 1988, 333, (6173), 562–5. [PubMed: 3287177]

27. Miyamoto N; Maki T; Shindo A; Liang AC; Maeda M; Egawa N; Itoh K; Lo EK; Lok J; Ihara M; Arai K, Astrocytes Promote Oligodendrogenesis after White Matter Damage via Brain-Derived Neurotrophic Factor. J Neurosci 2015, 35, (41), 14002–8. [PubMed: 26468200]

28. Maki T; Choi YK; Miyamoto N; Shindo A; Liang AC; Ahn BJ; Mandeville ET; Kaji S; Itoh K; Seo JH; Gelman IH; Lok J; Takahashi R; Kim KW; Lo EH; Arai K, A-Kinase Anchor Protein 12 Is Required for Oligodendrocyte Differentiation in Adult White Matter. Stem cells 2018.

29. Rubtsov N; Senger G; Kuzcera H; Neumann A; Kelbova C; Junker K; Beensen V; Claussen U, Interstitial deletion of chromosome 6q: precise definition of the breakpoints by microdissection, DNA amplification, and reverse painting. Hum Genet 1996, 97, (6), 705–9. [PubMed: 8641683]

30. Eash D; Waggoner D; Chung J; Stevenson D; Martin CL, Calibration of 6q subtelomere deletions to define genotype/phenotype correlations. Clin Genet 2005, 67, (5), 396–403. [PubMed: 15811006]

31. Ronzoni L; Tagliaferri F; Tucci A; Baccarin M; Esposito S; Milani D, Interstitial 6q25 microdeletion syndrome: ARID1B is the key gene. Am J Med Genet A 2016, 170A, (5), 1257–61. [PubMed: 26754677]

32. Michelson M; Ben-Sasson A; Vinkler C; Leshinsky-Silver E; Netzer I; Frumkin A; Kivity S; Lerman-Sagie T; Lev D, Delineation of the interstitial 6q25 microdeletion syndrome: refinement of the critical causative region. Am J Med Genet A 2012, 158A, (6), 1395–9. [PubMed: 22585544]

33. Thienpont B; Zhang L; Postma AV; Breckpot J; Tranchevent LC; Van Loo P; Mollgard K; Tommerup N; Bache I; Tumer Z; van Engelen K; Menten B; Mortier G; Waggoner D; Gewillig M; Moreau Y; Devriendt K; Larsen LA, Haploinsufficiency of TAB2 causes congenital heart defects in humans. Am J Hum Genet 2010, 86, (6), 839–49. [PubMed: 20493459]

34. Bisgaard AM; Kirchhoff M; Tumer Z; Jepsen B; Brondum-Nielsen K; Cohen M; Hamborg-Petersen B; Bryndorf T; Tommerup N; Skovby F, Additional chromosomal abnormalities in patients with a previously detected abnormal karyotype, mental retardation, and dysmorphic features. Am J Med Genet A 2006, 140, (20), 2180–7. [PubMed: 16955412]

35. Su PH; Chen JY; Chen SJ; Yang KC, Terminal deletion of chromosome 6q. Pediatr Neonatol 2008, 49, (3), 88–93. [PubMed: 18947005]

36. Sukumar S; Wang S; Hoang K; Vanchiere CM; England K; Fick R; Pagon B; Reddy KS, Subtle overlapping deletions in the terminal region of chromosome 6q24.2-q26: three cases studied using FISH. Am J Med Genet 1999, 87, (1), 17–22. [PubMed: 10528241]

37. Meng J; Fujita H; Nagahara N; Kashiwai A; Yoshioka Y; Funato M, Two patients with chromosome 6q terminal deletions with breakpoints at q24.3 and q25.3. Am J Med Genet 1992, 43, (4), 747–50. [PubMed: 1621768]

38. Meloni VA; Guilherme RS; Oliveira MM; Migliavacca M; Takeno SS; Sobreira NL; de Fatima Faria Soares M; de Mello CB; Melaragno MI, Cytogenomic delineation and clinical follow-up of two siblings with an 8.5 Mb 6q24.2-q25.2 deletion inherited from a paternal insertion. Am J Med Genet A 2014, 164A, (9), 2378–84. [PubMed: 24898331]

39. Nowaczyk MJ; Carter MT; Xu J; Huggins M; Raca G; Das S; Martin CL; Schwartz S; Rosenfield R; Waggoner DJ, Paternal deletion 6q24.3: a new congenital anomaly syndrome associated with intrauterine growth failure, early developmental delay and characteristic facial appearance. Am J Med Genet A 2008, 146A, (3), 354–60. [PubMed: 18203180]

40. Pirola B; Bortotto L; Giglio S; Piovan E; Janes A; Guerrini R; Zuffardi O, Agenesis of the corpus callosum with Probst bundles owing to haploinsufficiency for a gene in an 8 cM region of 6q25. J Med Genet 1998, 35, (12), 1031–3. [PubMed: 9863602]

41. Kratzer I; Chip S; Vexler ZS, Barrier mechanisms in neonatal stroke. Front Neurosci 2014, 8, 359. [PubMed: 25426016]

42. Maki T; Maeda M; Uemura M; Lo EK; Terasaki Y; Liang AC; Shindo A; Choi YK; Taguchi A; Matsuyama T; Takahashi R; Ihara M; Arai K, Potential interactions between pericytes and oligodendrocyte precursor cells in perivascular regions of cerebral white matter. Neurosci Lett 2015, 597, 164–9. [PubMed: 25936593]

43. Seo JH; Maki T; Maeda M; Miyamoto N; Liang AC; Hayakawa K; Pham LD; Suwa F; Taguchi A; Matsuyama T; Ihara M; Kim KW; Lo EH; Arai K, Oligodendrocyte precursor cells support blood-

brain barrier integrity via TGF-beta signaling. PLoS One 2014, 9, (7), e103174. [PubMed: 25078775]

44. Ronaldson PT; Davis TP, Blood-brain barrier integrity and glial support: mechanisms that can be targeted for novel therapeutic approaches in stroke. Curr Pharm Des 2012, 18, (25), 3624–44. [PubMed: 22574987]

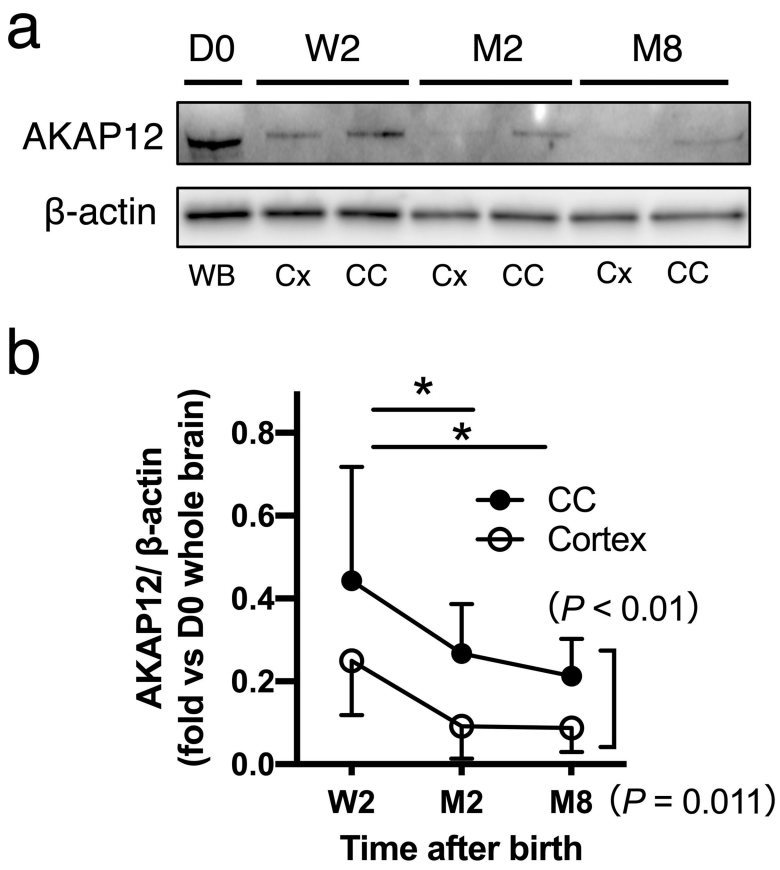

Figure 1. Spatio-temporal profile of AKAP12 expression in mouse brain after birth:

Western blotting analysis of the tissue lysates of whole brain samples (D0) and the lysates of corpus callosum (CC) or cortex (CX) samples (W2, M2 and M8) from WT, *Akap12*$^{+/-}$, and *Akap12*$^{-/-}$ mice. **(a)** Representative western blot images for AKAP12 band and β-actin band. **(b)** Quantitative results of western blot experiments. Significant Tissue × Time course interaction was not observed ($F_{(2, 24)} = 0.15$, P = 0.86). The levels of AKAP12 expression were significantly higher in the corpus callosum compared to in the cortex from postnatal 2-week to 8-month ($F_{(1, 24)} = 9.84$, P < 0.01; Two-way ANOVA). AKAP12 expression in postnatal 2-week old mice was also significantly higher compared to that of 2- and 8-month old mice (P = 0.011; Two-way ANOVA, *P < 0.05; Tukey's multiple comparison). WB; whole brain, Cx; cerebral cortex, CC; corpus callosum. D0; postnatal day 0, W2; postnatal 2-week, M2; postnatal 2-month, M8; postnatal 8-month. n = 4 per time point. Data are shown as mean plus and/or minus S.D.

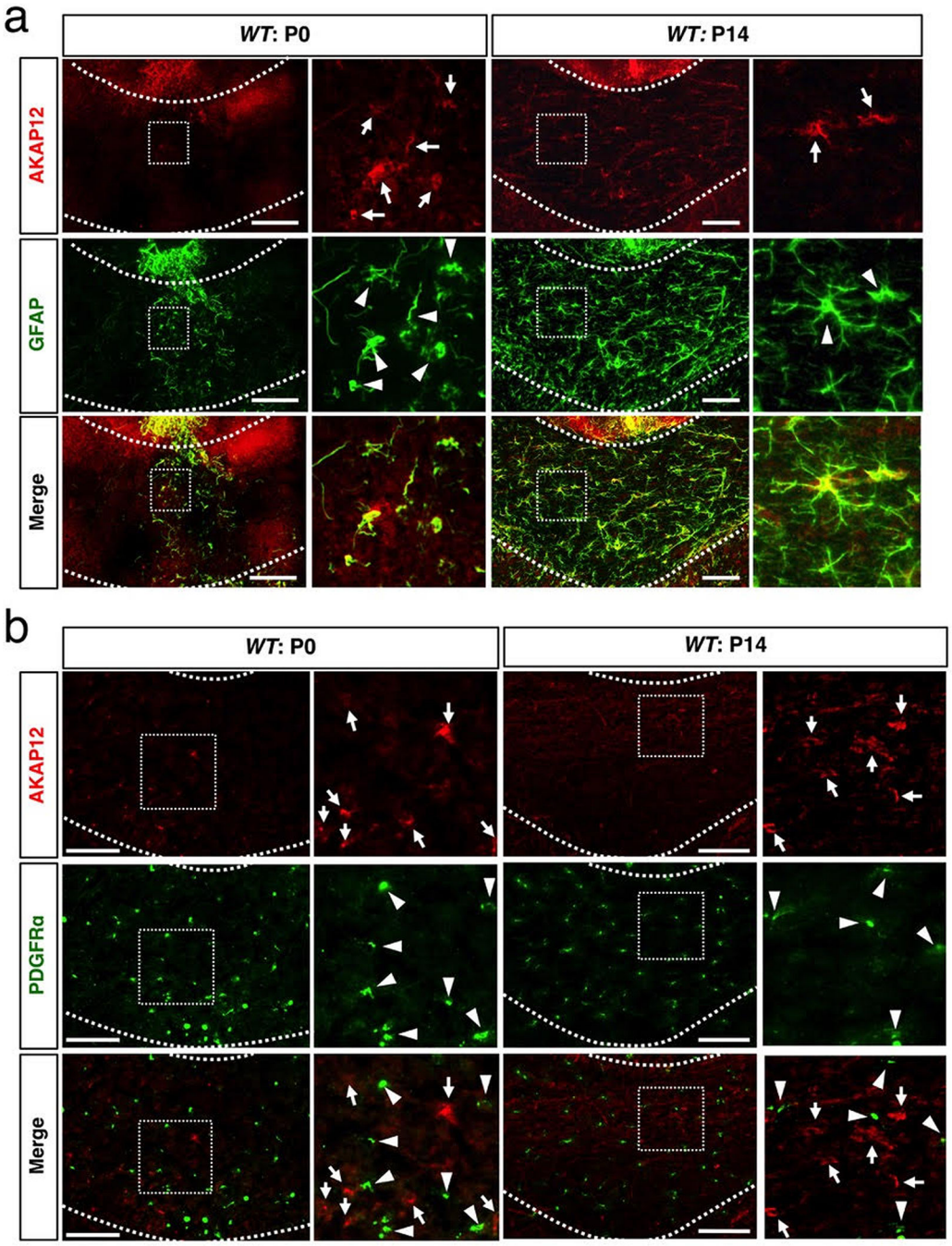

Figure 2. AKAP12 expression in postnatal corpus callosum:

AKAP12 (red; arrows) was expressed in the corpus callosum on postnatal days 0 (P0) and 14 (P14), and merged with GFAP (green; arrowheads) signals **(a)** but not with PDGFRα (green; arrowheads) positive cells **(b)** in WT mice. n = 3 on both P0 and P14. Scale bar = 100 μm

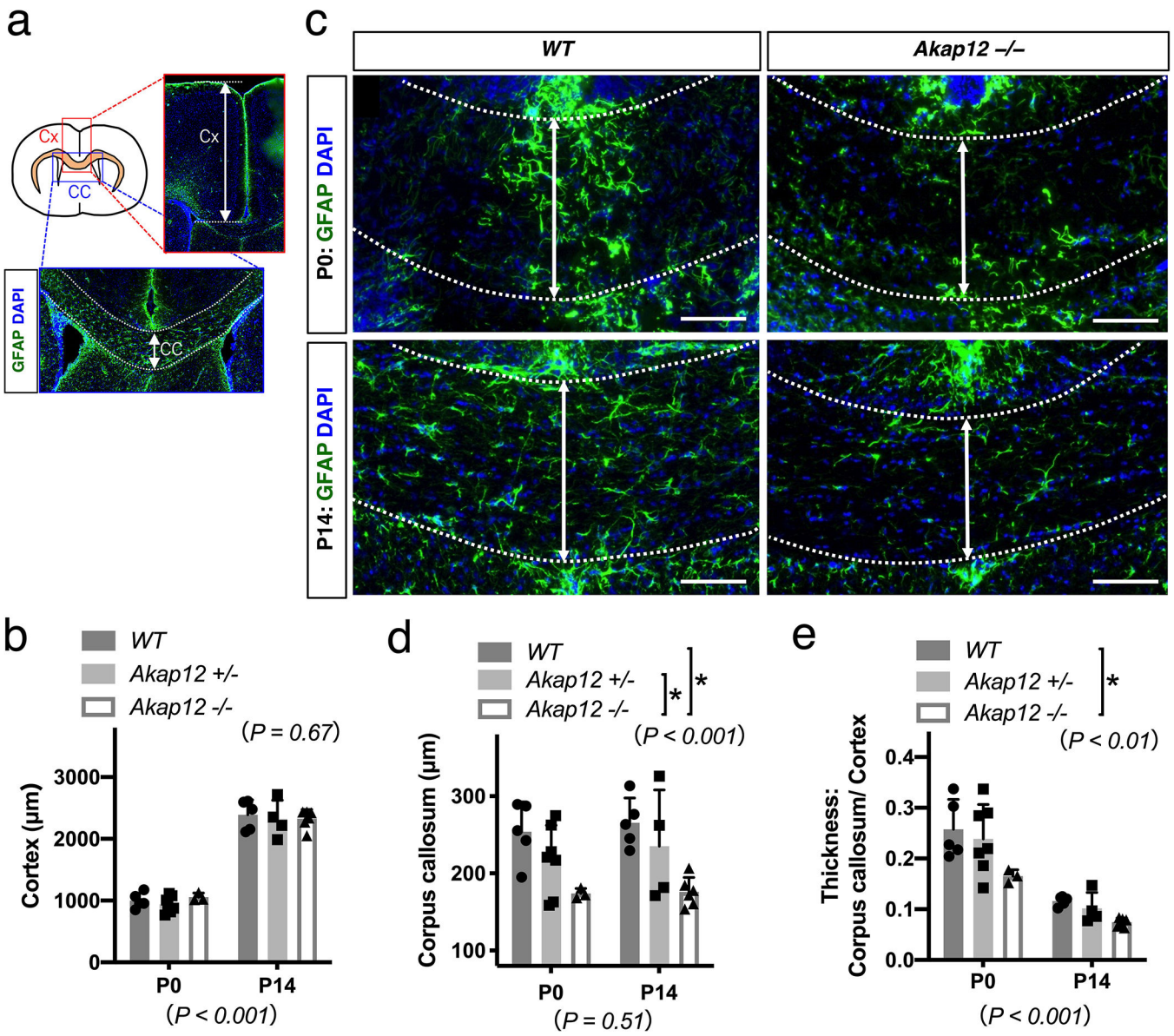

Figure 3. AKAP12 contributes to corpus callosum formation after birth:

(**a**) Schematic and representative images of GFAP (green) and DAPI (blue) staining of coronal brain sections on postnatal days 0 (P0) and 14 (P14). (**b**) In the analysis of cortical thickness, no significant Genotype × Time course interactions were observed ($F_{(2, 24)}$ = 0.29, P = 0.75). In addition, the cortical thickness was not significantly different between the 3 genotypes on P0 and P14 (P = 0.67; Two-way ANOVA); however, the cortical thickness was significantly different between P0 and P14 (P < 0.001; Two-way ANOVA). (**c, d**) In the analysis of callosal thickness, no significant Genotype × Time course interactions were observed ($F_{(2, 24)}$ = 0.079, P = 0.92). Callosal thickness was significantly greater in WT mice compared to *Akap12* heterozygous (*Akap12*$^{+/-}$) and homozygous (*Akap12*$^{-/-}$) KO mice (P < 0.001; Two-way ANOVA, *P < 0.05; Tukey's multiple comparison) and was not statistically different between P0 and P14 (P = 0.51; Two-way ANOVA). (**e**) The ratio between callosal thickness and cortex thickness showed no significant Genotype × Time

course interactions ($F_{(2, 24)}$ = 0.90, P = 0.42); however, the ratio in WT mice was significantly larger compared to that of *Akap12*$^{-/-}$ mice (P < 0.01; Two-way ANOVA, *P < 0.05; Tukey's multiple comparison). Furthermore, the ratio between callosal thickness and cortex thickness significantly decreased from P0 to P14 (P < 0.001; Two-way ANOVA). WT (P0; n = 5, P14; n = 5), *Akap12*$^{+/-}$ (P0; n = 7, P14; n = 4), *Akap12*$^{-/-}$ (P0; n = 3, P14; n = 5). Cx; cerebral cortex, CC; corpus callosum, Scale bar = 100 μm. Data are shown as mean plus S.D..

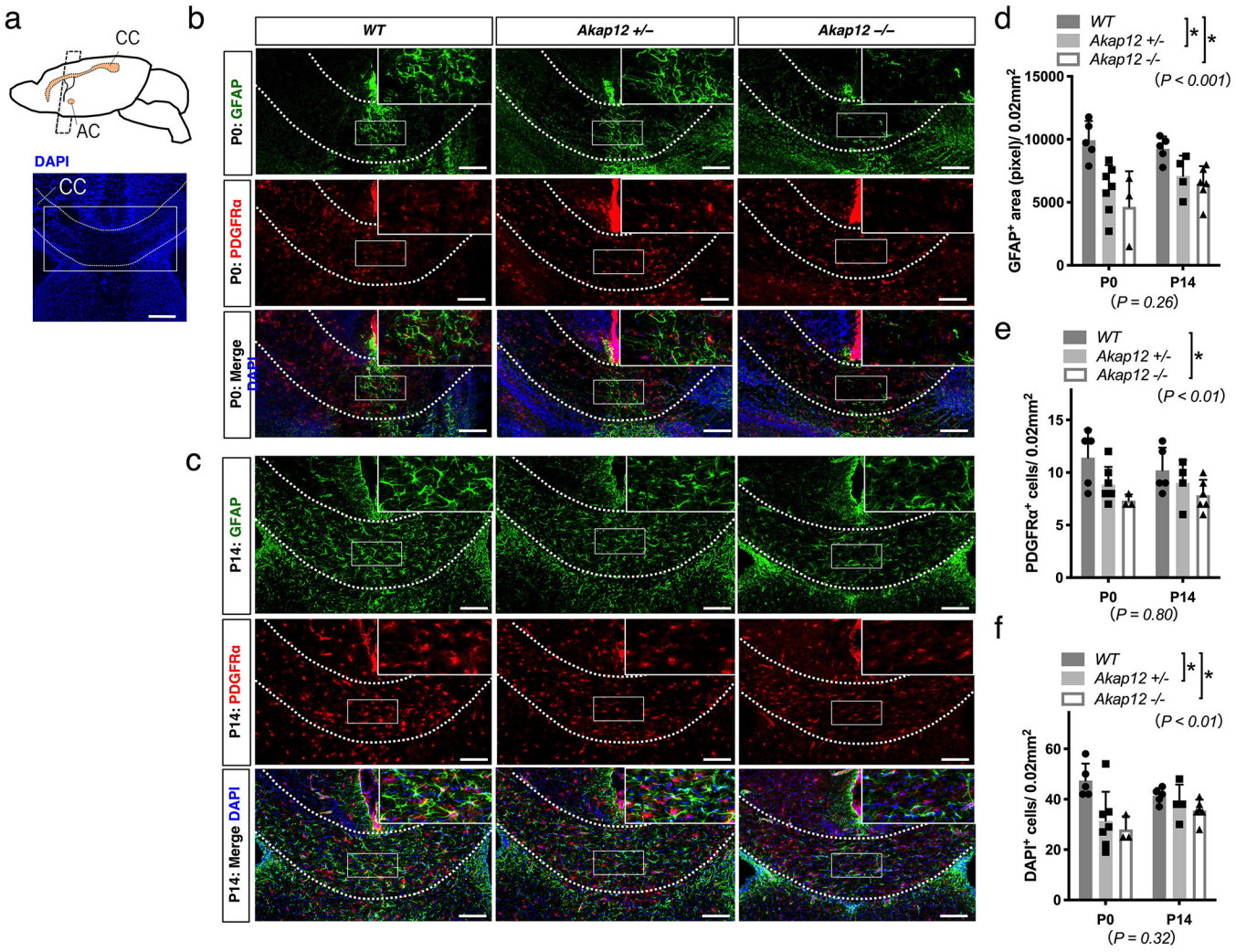

Figure 4. AKAP12 contributes to cell proliferation of astrocytes and OPCs in postnatal corpus callosum:

Immunofluorescences for GFAP (green), PDGFRα (red) and DAPI (blue) on coronal brain sections on postnatal day 0 (P0) and 14 (P14). (**a**; upper) Schematic diagram of mouse brain. Coronal brain sections at the level of anterior third of corpus callosum with circle shape of AC were analyzed. (**a**; lower) Representative DAPI staining (blue) image in the coronal section. (**b-d**) GFAP staining (green) demonstrated no significant Genotype × Time course interactions ($F_{(2, 24)}$ = 1.32, P = 0.29). The number of GFAP-positive astrocytes in WT mice was significantly larger than that of *Akap12* heterozygous (*Akap12*$^{+/-}$) and homozygous (*Akap12*$^{-/-}$) KO mice (P < 0.001; Two-way ANOVA, *P < 0.05; Tukey's multiple comparison). No significant difference was found between P0 and P14 (P = 0.26; Two-way ANOVA). (**b**, **c, e**) In the number of PDGFRα-positive OPCs, there were no significant Genotype × Time course interactions ($F_{(2, 24)}$ = 0.50, P = 0.61). The number of OPCs in WT mice was significantly larger than that of *Akap12*$^{-/-}$ mice (P < 0.01; Two-way ANOVA, *P < 0.05; Tukey's multiple comparison). No significant difference was observed between P0 and P14 (P = 0.80; Two-way ANOVA). (**b**, **c, f**) There were no significant Genotype × Time course interactions in DAPI number in the corpus callosum ($F_{(2, 24)}$ = 2.56, P = 0.10).

WT mice showed larger numbers of DAPI-positive cells than *Akap12*$^{+/-}$ and *Akap12*$^{-/-}$ mice ($P < 0.01$; Two-way ANOVA, $^{*}P < 0.05$; Tukey's multiple comparison). No statistical difference was found between P0 and P14 ($P = 0.32$; Two-way ANOVA). In the GFAP/PDGFRα double-staining images, there were no cells that were positive for both GFAP and PDGFRα. WT (P0; n = 5, P14; n = 5), *Akap12*$^{+/-}$ (P0; n = 7, P14; n = 4), *Akap12*$^{-/-}$ (P0; n = 3, P14; n = 5). CC; corpus callosum, AC; anterior commissure, LV; lateral ventricle, Scale bar = 100 μm. Data are shown as mean plus S.D.